https://doi.org/10.5194/egusphere-2023-1835
Preprint. Discussion started: 22 September 2023

An overview of organic aerosols at an urban site in Hong Kong: insights from in-situ measurement of molecular markers

Hongyong Li[1,2], Xiaopu Lyu[2*], Likun Xue[1*], Yunxi Huo[3], Dawen Yao[3], Haoxian Lu[4], Hai Guo[3*]

[1]Environment Research Institute, Shandong University, Qingdao, 266237, China
[2]Department of Geography, Faculty of Social Sciences, Hong Kong Baptist University, Hong Kong
[3]Department of Civil and Environmental Engineering, The Hong Kong Polytechnic University, Hong Kong
[4]Marine Biological Resources Bank, Southern Marine Science and Engineering Guangdong Laboratory (Zhuhai), Guangdong, China

Correspondence to: Xiaopu Lyu (xiaopu_lyu@hkbu.edu.hk); Likun Xue (xuelikun@sdu.edu.cn); Hai Guo (hai.guo@polyu.edu.hk)

Abstract. Organic aerosol (OA) is a significant constituent of urban particulate matter (PM), and molecular markers therein provide information on sources and formation mechanisms of OA. With in-situ measurement of over 70 OA molecular markers at a bihourly resolution, this study focused on the temporal variations of representative markers and dynamic source contributions to OA at an urban site in Hong Kong. The levels of secondary OA (SOA) markers were markedly elevated in continental and coastal air, and the primary markers were more of local characteristics. The diurnal patterns of 2-methyltetrols differed between scenarios, and their aqueous formation at night seemed plausible, particularly in the presence of troughs. Seven unambiguous sources were identified for the organic matters in submicron PM (PM_1-OM). Despite an urban site, the SOA contribution (49 ± 8%), primarily anthropogenic, was significant. Anthropogenic SOA dominated in continental and coastal air and in early afternoon. Local cooking and vehicle emissions became predominant in the scenario of marine air without troughs. Even averaged over the study period, cooking emissions contributed up to 40% to PM_1-OM in the early evening. The study highlighted the need to control regional anthropogenic SOA and local cooking emissions to mitigate PM pollution in Hong Kong.

Keywords: Organic aerosol; Molecular marker; Source apportionment; Cooking emissions; Anthropogenic secondary organic aerosol

1 Introduction

Atmospheric particulate matter (PM) has been a widespread environmental concern, due to its significant climate and health effects (Ramanathan et al., 2001; Poschl, 2005; Yang et al., 2018). Organic aerosols (OA) make up 20-90% of fine PM ($PM_{2.5}$) by mass concentration (Kanakidou et al., 2005; Jimenez et al., 2009). While the inorganic PM compositions are somewhat being effectively controlled, reducing OA remains a major challenge for further mitigation of $PM_{2.5}$ pollution in China (Huang et al., 2014; Zhang et al., 2019). This is closely related to the lag and inadequacy of our knowledge of OA, especially the

https://doi.org/10.5194/egusphere-2023-1835
Preprint. Discussion started: 22 September 2023

insufficient understanding of time-resolved and unambiguous identification of OA sources and SOA formation mechanisms. Therefore, it becomes increasingly important to improve the understanding of OA with new theories and techniques.

Molecular information records history of OA, including sources and chemical evolutions. Filter-based technique is a widely used method for measuring molecular compositions of OA (Yu et al., 2011; Ding et al., 2015; Fu et al., 2016). It generally takes half a day to a few days to collect PM on filters, followed by solvent or thermal extraction of target compounds and chemical analysis. However, during the collection cycle of each sample, emissions of OA and its precursors are not necessarily consistent, and chemical transformation may occur over several generations. For example, cooking and vehicle emissions vary significantly over the course of a day (Sun et al., 2018; Yao et al., 2021). With much higher time resolutions, Aerosol Mass Spectrometry (AMS) was developed and has been extensively applied in OA research (Sun et al., 2018; Liu et al., 2019; Yao et al., 2022). Nevertheless, AMS cannot provide molecular information of OA due to the application of hard ionization, which makes it difficult to identify unambiguous OA sources with AMS data (Sun et al., 2011; Lee et al., 2013). Applied earlier in the United States (Williams et al., 2006, 2010), in-situ measurement of OA molecular markers based on thermal desorption has become an emerging technique for chemical characterization of OA in China, *e.g.*, Beijing (Ren et al., 2019), Shanghai (Li et al., 2020; Wang et al., 2020), and Hong Kong (Lyu et al., 2020; Wang et al., 2022).

Hong Kong (HK) is a metropolis in East Asia with a developed economy and a high population density. Although the $PM_{2.5}$ level continued to decrease in recent decades, it is still far from the World Health Organization guideline value (5 μg m^{-3}). Led by the tertiary industry, HK has few high-emission industries. Street-level air pollution has long been a concern due to vehicle emissions (Lee et al., 2006; Huang et al., 2014; Liu et al., 2017a). Besides, mounting evidence demonstrates the considerable contributions of cooking emissions to OA (Lee et al., 2015; Sun et al., 2016). On the other hand, SOA formation in HK may also be significant, as mediated by the subtropical climate and coastal features. For example, studies indicated that aqueous processes accelerated SOA formation in spring with high relative humidity in HK (Li et al., 2013). In addition to local emissions and chemistry, transboundary transport also increases the atmospheric load of OA in HK (Huang et al., 2014; Lyu et al., 2017). With filter-based techniques, a range of molecular compositions of OA, such as polycyclic aromatic hydrocarbons (PAHs) (Guo et al., 2003; Liao et al., 2020), alkanes (Yao et al., 2004; Yu et al., 2011), dicarboxylic acids Ho et al., 2006; Hu et al., 2013), and anhydrosugars (Zhang et al., 2012; Ho et al., 2014), have been well studied in HK. Further, OA sources have also been explored by introducing the molecular markers into receptor models (Hu et al., 2010; Huang et al., 2014; Chow et al., 2022). Cooking emissions, vehicle emissions, biomass burning, and secondary formation were identified as the main sources of PM in Hong Kong. AMS has also been applied in HK, advancing our understanding of the dynamic features of OA and its sources (Lee et al., 2015; Xing et al., 2022). In recent years, Thermal desorption Aerosol Gas chromatography coupled with mass spectrometry (TAG) allowed in-situ measurement of OA molecular markers and facilitated understanding of dynamic source contributions to OA at two background sites in HK (Lyu et al., 2020; Wang et al., 2022). In brief, it was found that the concentrations of SOA tracers were significantly elevated in $PM_{2.5}$ pollution episodes, and transboundary transport led to a rise in biomass burning contributions to OA. Despite the previous studies, there is a lack of knowledge on time-resolved and unambiguous sources of OA in urban areas of HK.

https://doi.org/10.5194/egusphere-2023-1835
Preprint. Discussion started: 22 September 2023

This study presents the temporal variations of OA and a range of molecular markers therein based on a continuous measurement for ~1 month at an urban site in HK with TAG and AMS. Diurnal patterns of typical markers are discussed to indicate the emission patterns and possible formation mechanisms of OA. Source apportionment with the time-resolved data reveals the dynamic source contributions. The study enhances our understanding of urban OA in HK at bihourly resolution and molecular level, and provides a reference for PM pollution mitigation by intervention in OA emissions and formation.

2 Methods

2.1 Sampling campaign

The observation experiment was carried out in the campus of the Hong Kong Polytechnic University from June 6th to 26th in 2019. The instruments were deployed in a laboratory on 11th floor with a height of ~45 m above ground level. The sampling inlet protruded ~1.5 m from the wall. As shown in Figure 1, the site was in a mixed residential and commercial area with intensive traffic, which was also one of the areas with the highest concentration of restaurants in HK. Besides, it is worth noting that the nearby funeral parlors and temples within 1 km to the east of the site often conducted the burning of worship supplies, ritual candles, and incenses.

Despite an urban site, air pollution could also be influenced by regional transport. The 72-h backward trajectories of air masses reaching the site were calculated using the Hybrid Single Particle Lagrangian Integrated Trajectory model, which was driven by the Global Data Assimilation System archive data at the horizontal resolution of 1°×1°. The trajectories started from the location 50 m above the sampling site and were calculated every 2 hours. Based on their origins and paths, the air masses were classified into three types (Figure 1). Those from the South China Sea represented the marine air (blue trajectories in Figure 1) and accounted for ~87% of the total air masses. The rest included continental air (red) originating from and passing over the Mainland China (6%) and coastal air (orange) that arrived in HK along the coastlines of eastern and southern China (7%).

To analyze OA in small particles of interest, a submicron particulate matter (PM_1) cyclone was installed at the front of the inlet line made of pre-cleaned copper tubing. The cut-off size of 1μm also matched the design of the High Resolution − Time of Flight − Aerosol Mass Spectrometer (HR-Tof-AMS, referred to as AMS hereinafter) manufactured by Aerodyne Research Inc. The AMS couples size-resolved particle sampling and mass spectrometry analysis, enabling real-time measurement of non-refractory compositions of PM_1, including total organic matter (PM_1-OM), sulfate, nitrate, ammonium, and chloride. With hard ionization and in absence of species separation, AMS only provides mass spectral fragmentation information of size-segregated particles that arrive at the ionizer at the same time. As an important addition, the molecular markers of PM_1-OM were measured every 2 hours using the first commercialized TAG jointly developed by Aerodyne Research Inc and University of California, Berkeley. The main difference between TAG and traditional gas chromatography – mass spectrometry (GC-MS) is that TAG automates sample collection, derivatization, transfer, and GC-MS analysis. Within each cycle, the air after the removal of gaseous organics by a charcoal denuder was drawn and impacted onto a collection and thermal desorption (CTD) unit at a constant rate of ~10 L/min in the first 90 minutes. Afterwards, the CTD was heated according to a preset program. At

https://doi.org/10.5194/egusphere-2023-1835
Preprint. Discussion started: 22 September 2023

the same time, a helium flow saturated with N-Trimethylsilyl-N-methyl trifluoroacetamide was injected into the CTD to derivatize and purge the sample to a focusing trap (FT) that was maintained at room temperature. The FT allowed the volatiles to flow out and trapped the less-volatile compounds. Then, it was heated quickly, and the trapped substances were flushed to the chromatographic column head by helium. Lastly, the GC-MS analysis was performed, which however did not take any additional time, because it happened simultaneous with sample collection. The sample treatment, transfer, and some other steps took 30 minutes, thereby 2 hours for a complete cycle. With online derivatization and thermal desorption, the TAG was capable of analyzing a wide range of polar and nonpolar organic compounds. A mixture of deuterated compounds was used as internal standards (IS) to track and correct the changes in instrument sensitivity. More details about the AMS and TAG operations can be found in our previous studies (Lyu et al., 2020; Huo et al., 2022).

Besides, the mixing ratios of inorganic trace gases, including sulfur dioxide (SO_2), carbon monoxide (CO), nitric oxide (NO), nitrogen dioxide (NO_2), and ozone (O_3) were continuously measured in the sampling period. The instruments are listed in Table S1, and more operation and quality control details have been presented elsewhere (Guo et al., 2013). In this study, the average mixing ratios of SO_2, CO, NO, NO_2, and O_3 were 2.1 ± 0.1 ppbv (mean ± 95% confidence interval, the same below), 282 ± 12 ppbv, 10.7 ± 1.9 ppbv, 20.2 ± 1.4 ppbv, and 9.3 ± 1.6 ppbv, respectively. We adopted the meteorological parameters measured by the Hong Kong Observatory at the King's Park Meteorological Station, which was ~870 m away from our sampling site. They include temperature (Temp), relative humidity (RH), wind speed (WS), wind direction (WD), and ultraviolet (UV). During the sampling period, the average Temp, RH, WS, and UV were 28.6 ± 0.2 °C, 82 ± 1.1%, 2.4 ± 0.1 m/s, and 18.1 ± 2.8 W/m^2, respectively. The prevailing winds were roughly consistent with the origins of air masses indicated by the backward trajectories. Liquid water content (LWC) in PM_1 was calculated in the same way as that adopted by Yao et al. (2022), using the Extended Aerosol Inorganics Model with Temp, RH, and inorganic ions in PM_1 as inputs. It varied in the range of 0.2 – 62.0 μg/m^3, with a mean of 7.5 ± 1.2 μg/m^3.

2.2 Processing of TAG data

A total of 225 bi-hourly samples were analyzed by TAG throughout the experiment, and 74 OA markers in the volatility range equivalent to C_{16} – C_{36} *n*-alkanes were identified based on their retention time and mass spectrums, especially the base ion (Lyu et al., 2020), as shown in Table S2. In brief, we identified a species from the TAG chromatogram based on the retention time of the base ion of authentic standard and confirmed it by searching the ion fragments in an expanded NIST mass spectral library. For a few samples, the fatty acids and oleic acid were not fully derivatized, likely due to their exceptionally high concentrations in cooking hours. Peak fitting and integration were performed to both the derivatized and underivatized forms of them. The peak areas of the target compounds were scaled by those of the corresponding ISs with similar structures and close retention time. The pairing of target compounds and ISs are the same as that adopted in Lyu et al. (2020). In this way, the temporal variations of the 74 OA markers were not related to the changes in instrument sensitivity. However, we ran out of the external standards in this sampling campaign, so the concentrations of the detected species were not quantified. Instead, the internal standard scaled peak areas (IS-scaled PA) of the target compounds are used for analysis in this study.

https://doi.org/10.5194/egusphere-2023-1835
Preprint. Discussion started: 22 September 2023

For ease of analysis, we first classified the detected compounds based on their common origins and chemical structures. Further, correlation analysis was performed among them, as shown in Figure 2. Moderate to good correlations were identified for some species within 7 groups, including common SOA tracers, dicarboxylic acids (DCA) & hydroxyl dicarboxylic acids (OHDCA), sugars & sugar alcohols, *n*-alkanes, fatty acids, aromatic acids, and PAHs. The coefficient of determination (R^2) was higher than 0.65 for the correlations between any pairs of 4-/5-ring PAHs. The variations of levoglucosan and mannosan were roughly consistent (R^2 = 0.69). Good correlations were identified within the subgroups of high molecular weight (C_{25} – C_{30}) and low molecular weight (C_{20} – C_{24}) *n*-alkanes, separately, but not between them. This likely resulted from the different sources of them, *e.g.*, vegetable wax and debris for the former and petroleum products for the latter (Kawamura et al., 2003; Simoneit et al., 2004; Kang et al., 2016a). Consistent variations were observed for OHDCA species. Some DCAs, such as succinic acid which is a known precursor of malic acid (Hu et al., 2013), also correlated well with OHDCA. The patterns of isoprene SOA tracers formed in low NO_x environment, *i.e.*, 2-methyltetrols (2-MTs) and C_5-alkenetriols (Claeys et al., 2004; Edney et al., 2005; Surratt et al., 2010), resembled each other (R^2 >0.74). Besides, there also existed some correlations between species of different groups, mainly due to co-emissions from cooking (oleic acid, fatty acids, fructose isomers, and azelaic acid) and biomass burning (vanillic acid (VA), 4-hydroxybenzoic acid (4-OHBA), and levoglucosan). Based on the correlations, we selected 18 OA markers as representatives of the whole in the following analyses, as highlighted in Figure 2 and Table S2. All the chemical and meteorological data with time resolution higher than TAG data were converted to bihourly averages for matching purposes where necessary.

2.3 Application of Positive Matrix Factorization (PMF) model

PMF has been widely used as a quantitative tool to understand air pollution sources (Hu et al., 2010; Wang et al., 2018; Dai et al., 2020). In this study, the EPA PMF v5.0 was used to perform the source apportionment for PM_1-OM. A total of 13 OA markers measured by TAG were used to indicate the sources, including 3 OHDCA species (MA, CMA, and 2-HGA, see Table S2 for the full names), 2 anthropogenic SOA tracers (DHOPA and phthalic acid), 3 isoprene SOA tracers (2-MT1, cis-2-MBT, and 2-MGA), and 5 primary organic aerosol (POA) species (levoglucosan, fructose-2, palmitic acid, norhopane, and oleic acid). The uncertainty file was compiled following the method described in Lyu et al. (2020), based on an error faction of 10% and method detection limit (MDL) for individual species. The MDL for PM_1-OM was determined to be 0.201 μg/m^3. The MDLs of OA species were taken from Lyu et al., (2020) that used the same TAG ~8 months earlier. For the newly detected species, *e.g.*, phthalic acid, 2-MGA, cis-2-MBT, and norhopane, we assume 10% of the averages as the MDLs. Extreme values are generally difficult to be reproduced by PMF model, especially for data points with scaled residuals greater than 4. To address this, greater weight was given to the high values that are considered true in the PMF iteration process, as described by Wang et al. (2018).

The optimal number of PMF factors was determined according to the mathematical tests and physical interpretability. We examined the solutions with 3 – 10 factors and the corresponding Q/Qexp ratios (Figure S1). The ratio decreased rapidly for 3 – 7 factors and the decline slowed down for 7 – 10 factors, demonstrating a minimum of 7 factors from a mathematical

https://doi.org/10.5194/egusphere-2023-1835
Preprint. Discussion started: 22 September 2023

perspective. Further inspections found that some tracers indicative of different sources (*e.g.*, DHOPA and MA) were not separated in the 7-factor solution, and some species were not well reproduced. The 9-factor solution however apportioned tracers of a same source into multiple factors. We ended up with 8 factors, which provided reasonably good fit for all species with physically interpretable source profiles.

3 Results and Discussion

3.1 Overview of the sampling campaign

Figure 3 and Figure S2 show the time series of the selected OA markers, PM_1 compositions, trace gases, and meteorological conditions throughout the sampling period. The origins of air masses are also labelled. The total organics, sulfate, nitrate, and ammonium in PM_1 were observed with the average concentration of 4.2 ± 0.5, 2.9 ± 0.3, 0.3 ± 0.1 and 1.1 ± 0.1 μg/m^3, respectively. The fraction of PM_1-OM (47.1 ± 2.2%) was slightly higher than that at an urban background site in HK (43.8%), but lower than that at a roadside site ~350 m away (57.7%) (Yao et al., 2021,2022). PM_1-OM had the highest concentration in the continental air, followed by that in coastal air and marine air, same for CO and O_3 (Table S3). However, the highest levels of sulfate and ammonium were observed in coastal air, likely due to aqueous aging of regional air pollution (Huo et al., 2023). Although the marine air was supposed to be relatively clean, it contained elevated levels of SO_2 and NO_x, which correlated well with each other (R^2 = 0.76). This phenomenon was in line with that at the three roadside sites in HK, but was not identified at the general urban sites (Figure S3). Therefore, the close relationship between SO_2 and NO_x on the days with marine air were likely attributable to local vehicle emissions rather than ship emissions. Moreover, the concentrations of many air pollutants, including both primary and secondary species, increased significantly on June 10th – 14th and 24th – 26th, when HK was affected by the troughs of low pressure with cloudy weather and low wind speed. This might be related to the unfavorable dispersion conditions and enhanced chemistry under special meteorological conditions, such as high RH. The effects also applied to some OA markers, such as malic acid and its homologues.

The cooking-related OA markers, such as oleic acid, palmitic acid, and fructose isomers, did not show obvious inclination toward the trough periods and exhibited some periodic spikes in the marine air. Therefore, it seemed that local cooking emissions somewhat overwhelmed the effects of atmospheric mixing and transformation. The lower levels of cooking markers in continental and coastal air could be partially explained by the quicker chemical losses, due to the higher concentrations of oxidants, *e.g.*, O_3 (Table S3). Oleic acid with a carbon-carbon double bond in the molecule can be efficiently oxidized by O_3 and other oxidants (Zeng et al., 2020; Wang et al., 2021). Differently, levoglucosan, pyrene, and some odd *n*-alkanes (*e.g.*, *n*-C_{27}) with a few spikes were more abundant in coastal air. Further, we found that high levels of levoglucosan were associated with easterly winds (Figure S4). As stated above, biomass product combustions were common within 1 km east of the site (Figure 1). Therefore, the observed variations of levoglucosan were mainly attributed to local emission patterns, different from the regional transport of biomass burning plumes from mainland to HK in cool seasons (Sang et al., 2011; Chow et al., 2015).

https://doi.org/10.5194/egusphere-2023-1835
Preprint. Discussion started: 22 September 2023

The wind dependence was not identified for others, except that the strong southwest winds caused low levels of many OA markers due to the dilution by marine air.

The temporal variations of secondary OA markers were quite different. The abundances of 2-MTs (*e.g.*, 2-MT1, see Table S2), C_5-alkenetriols (*e.g.*, *cis*-2-MBT), and 2-MGA increased significantly by 13.1, 18.4, and 13.8 times when the continental air arrived at the site. Consistent with that at an urban background site (Lyu et al., 2020), higher levels of 2-MTs (isoprene SOA in NO_x-lean environment) were observed at night and 2-MGA (isoprene SOA in NO_x-rich environment) exhibited the peak in the afternoon. The temperature and UV were not exclusively high on the days with continental air, and we presume the same for biogenic emissions locally. Therefore, the notable levels of isoprene SOA tracers on these days suggested that the continental air transported biogenic SOA and/or the precursors to HK. Succinic acid correlated fairly well with 2-MGA in the continental air (R^2 = 0.84, compared to R^2 of 0.56 at other times), indicating that it was a degradation product of isoprene under high-NO_x conditions. Besides, the first day with continental air also experienced highest levels of DHOPA and phthalic acid, two anthropogenic SOA tracers derived from aromatics (Bunce et al., 1997; Jang et al., 1997; Kleindienst et al., 2004). This could also be related to regional transport, given the notable rise in other anthropogenic air pollutants (*e.g.*, CO). In addition, it was likely that the enhancement of atmospheric oxidation capacity, as indicated by the highest level of O_3 over the sampling campaign, facilitated the formation of many SOA species on this day. These factors might also play a role in maintaining the high levels of OHDCA, such as malic acid and tartaric acid, which were elevated during a low-pressure trough in the previous days with marine air.

3.2 Diurnal patterns of representative OA markers

An advantage of TAG measurement is the time-resolved data of OA markers. Figure 4 presents the average diurnal profiles of 9 representative species, and some others with lower priorities are shown in Figure S5. As discussed above, the high levels of levoglucosan were related to the combustion of biomass products nearby. Here, we notice a small peak at 10:00 and a marked increase during 18:00 – 20:00 for levoglucosan. The pattern, especially the early evening peak, roughly coincided with the timing of smokes from the funeral parlor chimneys, according to our observations. Some other species, including 4-OHBA, VA, mannosan, xylose, hydroxybutyric acid, and protocatechuic acid showed consistent diurnal patterns (Figure S5), indicating that they were mainly derived from biomass burning. Besides, C_{26} – C_{31} *n*-alkanes were observed with distinct peaks at 8:00 and 20:00 and might also be influenced by nearby sacrificial activities. Other sources, *e.g.*, vehicle emissions, might also contribute to the morning peak that was more pronounced than levoglucosan. As an indicator of vehicle emissions, norhopane exhibited higher levels in daytime than at night, and were slightly elevated in the morning and evening rush hours. Similar diurnal patterns were observed for C_{20} – C_{23} *n*-alkanes (Figure S5), which could also be derived from vehicle emissions. Oleic acid was obviously enhanced at noon and in early evening, when intensive cooking activities took place in restaurants and at home, same for fatty acids, azelaic acid, and fructoses (Figure S5). Pyrene, as a representative of PAHs, got the highest level at 20:00. Interestingly, it correlated well with levoglucosan (R^2 = 0.88) at this point of time (Figure S6) and exhibited no correlation with oleic acid which also had the highest levels in the early evening. At the other times excluding 14:00 – 16:00

https://doi.org/10.5194/egusphere-2023-1835
Preprint. Discussion started: 22 September 2023

when photochemical reactions might consume a large fraction of NO_x, the variation of pyrene was consistent with that of NO_x ($R^2 = 0.70$). Therefore, the exhaust fume from nearby funeral parlors were responsible for the peak values of PAHs in the early evening, while the lower levels of PAHs were likely associated with vehicle emissions.

Contrary to the common understanding, the 2-MTs showed higher levels between midnight and dawn, same for C_5-alkenetriols. This however was in line with previous observations at two background sites in HK conducted by us and another team (Lyu et al., 2020; Wang et al., 2022). Day-by-day inspections found inconsistent diurnal patterns for 2-MTs, which were grouped into four categories, as shown in Figure 5. As speculated in previous studies (Lyu et al., 2020), the higher levels of 2-MTs in continental and coastal air might result from transboundary transport and diurnal evolution of boundary layer. On the days with marine air, two distinct patterns were identified. Similar night time enhancement was observed in the presence of troughs. Interestingly, 2-MTs exhibited the highest levels in the afternoon without the influence of the troughs. These days were accompanied by higher temperature and UV intensity, but lower RH and LWC (Figure 5). Therefore, the afternoon peak was likely attributed to the more intensive emissions and photochemical oxidation of isoprene. Moreover, we uncovered some clues that nocturnal chemistry might regulate the diurnal patterns of 2-MTs. According to Noziere et al. (2011), the ratio of 2-methylerythritol to the sum of 2-MTs (2-MT1/2-MTs) indicates the sources of 2-MTs: primary emissions (0.35), NO_x-lean photooxidation (0.61), NO_x-rich photooxidation (0.76), and aqueous phase oxidation (0.90). Under the assumption that the instrument sensitivity to the two 2-MT isomers were the same, the average 2-MT1/2-MTs ratio was 0.70 in the marine air without troughs. However, it was much higher (0.81) in presence of troughs, especially at night, in line with the patterns of LWC. Hence, the higher levels of 2-MTs at night might be related to aqueous chemistry. Nevertheless, it could not be the sole reason for the counterintuitive patterns of 2-MTs in continental and coastal air, where the average 2-MT1/2-MTs ratio was 0.76 and 0.77, respectively. The influence of other factors, such as transport and atmospheric mixing, deserves study.

Conversely, 2-MGA exhibited a typical diurnal pattern of photochemical pollution, increasing from morning to afternoon, except an exclusively high value at ~10:00 on one day with continental air. Daytime enhancements were also observed for DHOPA and phthalic acid, suggesting that photochemistry was involved in the formation of these SOA tracers. It is noteworthy that the peak of phthalic acid appeared at 12:00, ~4 hours earlier than the peaks of 2-MGA and DHOPA, which might be due to differences in formation mechanisms and/or oxidation states. For example, Yao et al. (2022) found that the peak of more oxidized oxygenated OA was several hours later than that of less oxidized OA, and aqueous processes were suspected between the two peaks. Despite a slight rebound at 12:00 – 14:00, the diurnal variation of malic acid was small, much less pronounced than that at an urban background site (Lyu et al., 2020). This pattern also applied to the other OHDCA species, which might be partially attributed to the lower atmospheric oxidation capacity, as reflected by the difference in odd oxygen ($O_x = O_3 + NO_2$) levels, *i.e.*, 29.5 ppbv at this site *vs.* 49.8 ppbv at the background site.

3.3 Source apportionment of PM_1-OM

Figure 6 shows the source profiles of the 8 factors resolved by PMF. Levoglucoan was assigned to multiple factors in the base run, although the factor of biomass burning accounted for the highest fraction. Constraint was applied to reduce the

https://doi.org/10.5194/egusphere-2023-1835
Preprint. Discussion started: 22 September 2023

levoglucosan loadings in other factors, thereby lower rotational ambiguity. Moreover, we also performed simulations without PM_1-OM that was measured by AMS. This was to examine if it was appropriate to mix the components measured by two different instruments in the source apportionment. As shown, the source profiles did not change much between these simulations. Table S4 summarizes the R^2, slope, and intercept for the linear regression between the simulated and observed values of individual species, which are in reasonable ranges. The scaled residuals for all the species were within the range of -3 to 3. These metrics indicated that the observed magnitudes and variations of the PMF species were well reproduced. To evaluate the model stability and uncertainty of the results, Bootstrapping (BS) and displacement (DISP) analyses were conducted. Based on BS tests, the factor mappings ranged from 85% to 100% except for an unresolved factor (77%), above the threshold of 80% representing robust factors recommended by the PMF user guide. Namely, there was no observation that disproportionately influenced the solution. Besides, no factor swap was found from the DISP analysis. The BS and DISP results indicated the robustness of the 8-factor solution. The unresolved factor is discussed below.

The 8 factors were identified as cooking emissions, vehicle emissions, biomass burning, isoprene SOA, anthropogenic SOA represented by phthalic acid (ASOA-1), anthropogenic SOA represented by DHOPA (ASOA-2), OHDCA-like SOA, and an unresolved factor. Factor 1 was dominated by oleic acid, palmitic acid, and fructose isomers, indicating the source of cooking emissions (To et al., 2000; Lyu et al., 2021; Huo et al., 2022). The second factor was regarded as vehicle emissions, due to the high loading of norhopane (Zielinska et al., 2004). Factor 3 with the dominance of levoglucosan signified biomass burning (Fabbri et al., 2009). Factor 4 was identified by 2-MT2 and cis-2-MBT, both of which were isoprene SOA tracers formed in NO_x-lean environments (Claeys et al., 2004). We define the fifth and sixth factor as ASOA-1 and ASOA-2 based on the highest percentage of phthalic acid and DHOPA, respectively, because phthalic acid and DHOPA have been shown to be oxidation products of aromatics (Bunce et al., 1997; Jang et al., 1997; Kleindienst et al., 2004). Factor 7 was characterized by its high contribution to MA and moderate contributions to CMA and 2-HGA, all of which were OHDCA species. Our previous studies (Lyu et al., 2020; Huo et al., 2023) indicated that OHDCA in HK was attributed to photochemical and aqueous processes rather than direct emissions, so this factor was termed as OHDCA-like SOA. With percentage contributions to all the species lower than 35%, the last factor could not be recognized through any indicative species. It had the smallest diurnal variation with a coefficient of variation of 0.75, compared to 1.17 – 4.42 for the other factors. Therefore, we presume this unresolved factor might be related to the background residue. As discussed below, this factor only contributed 9 ± 1% to PM_1-OM.

Further, the source contributions to PM_1-OM were determined. As shown in Figure 7a, they varied noticeably over time, underlining the value of source apportionment based on in-situ measurement of OA markers. Cooking emissions, vehicle emissions, ASOA-2, OHDCA-like SOA and ASOA-1 were the main sources of PM_1-OM, with the average contribution of 19 ± 3%, 18 ± 4%, 16 ± 4%, 15 ± 2%, 15 ± 3%, respectively. Biomass burning and isoprene SOA only accounted for 5 ± 2% and 4 ± 1% of PM_1-OM. This demonstrated the significant role of anthropogenic air pollution, either primary or secondary, in contributing to PM_1-OM at this urban site. However, biogenic contributions might be somewhat underestimated, because i) we failed to separate a source represented by 2-MGA, an isoprene SOA tracer formed in NO_x-rich environment; ii) OHDCA-like SOA could be formed through the oxidation of biogenic precursors (Hu et al., 2013; Huo et al., 2023); and iii) SOA tracers

https://doi.org/10.5194/egusphere-2023-1835
Preprint. Discussion started: 22 September 2023

derived from monoterpenes were not detected. The dominant sources, especially cooking and vehicle emissions, were different from those at the urban background site (Lyu et al., 2020), likely due to the depletion of primary emissions during the course of their airborne migration to the background site.

On the days with continental air, vehicle emissions and ASOA-2 with the contribution to PM_1-OM of 31 ± 18% and 32 ± 8% were the most predominant, while only 1 ± 1% of PM_1-OM was attributed to cooking emissions (Figure 7b). It is noteworthy that anthropogenic SOA, sum of ASOA-1 and ASOA-2, accounted for almost half (47 ± 12%) of PM_1-OM. The peaks were in sync with that of CO, suggesting that the enhancement of anthropogenic SOA was more likely due to transboundary transport. Similarly, vehicle emissions and ASOA-2 were also the leading sources in coastal air, contributing 30 ± 12% and 28 ± 6% to PM_1-OM, respectively. However, in the marine air scenario, cooking emissions (26 ± 5%, source contribution, the same below) ranked the largest source of PM_1-OM, followed by ASOA-1 (17 ± 4%), OHDCA-like SOA (15 ± 3%), and vehicle emissions (13 ± 2%). As discussed in section 3.1, some OA markers were elevated under the influence of the low-pressure troughs when backward trajectories still indicated marine air. Correspondingly, the contributions of ASOA-1 and OHDCA-like SOA to PM_1-OM increased to 26 ± 5% and 20 ± 3%, respectively. It was a bit surprising to note the rise in SOA contributions in these periods, because of the lower temperature and weaker UV (Figure 3). The growth of OHDCA-like SOA might be facilitated by the high RH and LWC through aqueous processes (Huo et al., 2023). While it is unknown whether this also caused the increase of ASOA-1, moderate correlation (R^2=0.41) was identified between phthalic acid and the product of RH and UV, which was not found at other times (Figure S7). Thus, the high RH might be one of the leading factors, if not all, of SOA enhancements in presence of troughs. In contrast, cooking emissions became the largest source of PM_1-OM (41 ± 9%) in the scenario of marine air without troughs, and in second place was vehicle emissions (14 ± 3%). This was more reflective of local emissions with less chemical aging. Overall, the SOA contributions increased significantly with the rise in PM_1-OM concentration (Figure S8), consistent with the findings at a suburban site that $PM_{2.5}$ pollution events witnessed a notable rise in SOA tracer levels (Wang et al., 2022). Moreover, the anthropogenic SOA might also be underestimated, similar to the situation with biogenic SOA. For example, cooking emissions were expected to be relatively consistent across days. The notable decline in continental and coastal air was likely a result of enhanced aging, due to the higher concentrations of oxidants, such as O_3 (Table S3). However, we have not identified a source of aged cooking emissions, although some fractions of it might have been allocated to the identified SOA factors, such as OHDCA-like SOA.

Furthermore, the diurnal variations of source contributions were also evident (Figure 7c). Cooking emissions were responsible for up to 40 ± 7% of PM_1-OM during 18:00 – 20:00. Almost at the same time, biomass burning also contributed 10 ± 5% to PM_1-OM, although it was on average a small source. Therefore, short-term exposure to emissions of these sources might be a concern, especially due to the fact that the highest levels of PAHs were related to biomass burning as discussed above. The total percentage contribution of SOA was relatively high and stable between 0:00 and 16:00, and decreased in the early evening as the cooking and biomass burning emissions intensified. The special diurnal pattern of total SOA contribution was a result of superposition of 4 SOA factors with different diurnal patterns, as shown in Figure S9. It is worth mentioning that the contribution of anthropogenic SOA could reach 40 ± 29% in the early afternoon (12:00 – 14:00).

https://doi.org/10.5194/egusphere-2023-1835
Preprint. Discussion started: 22 September 2023

4 Conclusion

As a ubiquitous composition of atmospheric fine PM, OA has been extensively studied. Nevertheless, it is still a major obstacle to further improving PM air quality in many places around the world, and also a meeting point in control of air pollution complex, such as $PM_{2.5}$ and O_3 in photochemical smog.

Taking advantage of an emerging technique for in-situ measurement of OA molecular markers, we reported by far the highest-resolution temporal variations of dozens of OA markers in a summer month in urban HK. The time-resolved data allowed to discuss the effects of transboundary transport and weather patterns (*e.g.*, troughs) on primary and secondary OA markers. DHOPA, phthalic acid, and isoprene SOA tracers were more enriched in the continental air, probably due to more abundant precursors and higher atmospheric oxidation capacity. The high RH brought on by troughs might have facilitated the formation of some OA species, such as OHDCA. Further, the diurnal variations of OA markers indicated emission patterns and SOA evolutions, such as the most intense cooking emissions in early evening and potentially enhanced 2-MTs formation in presence of troughs. Regarding the sources of PM_1-OM, we uncovered the dominance of cooking and vehicle emissions in the scenario of marine air without troughs, which was the cleanest case. Even as a whole, cooking emissions explained ~40% of the PM_1-OM in early evening. Anthropogenic SOA and vehicle emissions were the main sources of PM_1-OM in the continental and coastal air, and the SOA contributions, mainly from anthropogenic components, substantially increased when the PM air quality deteriorated. The findings demonstrated the need to properly manage local cooking and vehicle emissions and to control aromatics-derived SOA with concerted efforts on a regional or even superregional scale.

While this study provides valuable insights, we acknowledge there are several limitations. First, the molecular markers were not quantified, making it impossible to compare with the measurements elsewhere or compare among the detected species for absolute concentrations. It also hinders reuse of the data by other studies, such as concentration-based health risk assessment for some species. Second, some SOA tracers, such as those derived from monoterpenes and sesquiterpenes, were not detected. This increased the uncertainty of OA source apportionment to some extent. Third, we reiterated the unexpected diurnal patterns of 2-MTs, but the analysis of the underlying reasons is speculative. Therefore, future work will be dedicated to improving the analytical performance of TAG and exploring complex mechanisms responsible for unique features of SOA tracers, including 2-MTs.

Acknowledgements

This study was supported by the Hong Kong Research Grants Council (RGC) via the National Natural Science Foundation of China/RGC joint research scheme (N_PolyU530/20), the National Natural Science Foundation of China (42061160478), and the General Research Fund (HKBU 15219621). XL acknowledges the Tier 1 Research Start-up Grants provided by Hong Kong Baptist University (162912).

https://doi.org/10.5194/egusphere-2023-1835
Preprint. Discussion started: 22 September 2023

Author contributions

HL performed the study and drafted the manuscript. XL designed the study, oversaw interpretation of the results and revised the manuscript. YH, DY, and HL assisted in field campaign and processed relevant data. LX and HG led the project and revised the manuscript.

Data availability

All raw data are available upon request from the corresponding author Dr. Xiaopu Lyu.

Competing interests

The authors declare no competing interests.

References

Bunce, N. J., Liu, L., Zhu, J., and Lane, D. A.: Reaction of naphthalene and its derivatives with hydroxyl radicals in the gas phase, Environ. Sci. Technol., 31, 2252–2259, https://doi.org/10.1021/es960813g, 1997.

Cheng, Y., Ma, Y., and Hu, D.: Tracer-based source apportioning of atmospheric organic carbon and the influence of anthropogenic emissions on secondary organic aerosol formation in Hong Kong, Atmos. Chem. Phys., 21, 10589–10608, https://doi.org/10.5194/acp-21-10589-2021, 2021.

Chow, K. S., Huang, X. H. H., and Yu, J. Z.: Quantification of nitroaromatic compounds in atmospheric fine particulate matter in Hong Kong over 3 years: field measurement evidence for secondary formation derived from biomass burning emissions, Environ. Chem., 13, 665, https://doi.org/10.1071/EN15174, 2015.

Chow, W. S., Huang, X. H. H., Leung, K. F., Huang, L., Wu, X., and Yu, J. Z.: Molecular and elemental marker-based source apportionment of fine particulate matter at six sites in Hong Kong, China, Sci. Total Environ., 813, 152652, https://doi.org/10.1016/j.scitotenv.2021.152652, 2022.

Claeys, M., Graham, B., Vas, G., Wang, W., Vermeylen, R., Pashynska, V., Cafmeyer, J., Guyon, P., Andreae, M. O., Artaxo, P., and Maenhaut, W.: Formation of secondary organic aerosols through photooxidation of isoprene, Science, 303, 1173–1176, https://doi.org/10.1126/science.1092805, 2004.

Dai, Q., Liu, B., Bi, X., Wu, J., Liang, D., Zhang, Y., Feng, Y., and Hopke, P. K.: Dispersion normalized PMF provides insights into the significant changes in source contributions to $PM_{2.5}$ after the COVID-19 outbreak, Environ. Sci. Technol., 54, 9917–9927, https://doi.org/10.1021/acs.est.0c02776, 2020.

https://doi.org/10.5194/egusphere-2023-1835
Preprint. Discussion started: 22 September 2023

Ding, X., Wang, X. M., Gao, B., Fu, X. X., He, Q. F., Zhao, X. Y., Yu, J. Z., and Zheng, M.: Tracer-based estimation of secondary organic carbon in the Pearl River Delta, south China, J. Geophys. Res.-Atmos., 117, 1–14, https://doi.org/10.1029/2011JD016596, 2012.

Edney, E. O., Kleindienst, T. E., Jaoui, M., Lewandowski, M., Offenberg, J. H., Wang, W., and Claeys, M.: Formation of 2-methyl tetrols and 2-methylglyceric acid in secondary organic aerosol from laboratory irradiated isoprene/NOX/SO 2/air mixtures and their detection in ambient $PM_{2.5}$ samples collected in the eastern United States, Atmos. Environ., 39, 5281–5289, https://doi.org/10.1016/j.atmosenv.2005.05.031, 2005.

Fabbri, D., Torri, C., Simoneit, B. R., Marynowski, L., Rushdi, A. I., Fabianska, M. J.: Levoglucosan and other cellulose and lignin markers in emissions from burning of Miocene lignites, Atmos. Environ., 43, 2286−2295, https://doi.org/10.1016/j.atmosenv.2009.01.030, 2009.

Fu, P., Aggarwal, S. G., Chen, J., Li, J., Sun, Y., Wang, Z., Chen, H., Liao, H., Ding, A., and Umarji, G. S.: Molecular markers of secondary organic aerosol in Mumbai, India, Environ. Sci. Technol., 50, 4659–4667, https://doi.org/10.1021/acs.est.6b00372, 2016.

Guo, H., Lee, S. C., Ho, K. F., Wang, X. M., and Zou, S. C.: Particle-associated polycyclic aromatic hydrocarbons in urban air of Hong Kong, Atmos. Environ., 37, 5307–5317, https://doi.org/10.1016/j.atmosenv.2003.09.011, 2003.

Ho, K. F., Lee, S. C., Cao, J. J., Kawamura, K., Watanabe, T., Cheng, Y., and Chow, J. C.: Dicarboxylic acids, ketocarboxylic acids and dicarbonyls in the urban roadside area of Hong Kong, Atmos. Environ., 40, 3030-3040, https://doi.org/10.1016/j.atmosenv.2005.11.069, 2006.

Ho, K. F., Engling, G., Ho, S. S. H., Huang, R. J., Lai, S. C., Cao, J. J., and Lee, S. C.: Seasonal variations of anhydrosugars in $PM_{2.5}$ in the Pearl River Delta Region, China, Tellus B, 66, 22577, https://doi.org/10.3402/tellusb.v66.22577, 2014.

Hu, D., Bian, Q., Lau, A. K. H., and Yu, J. Z.: Source apportioning of primary and secondary organic carbon in summer $PM_{2.5}$ in Hong Kong using positive matrix factorization of secondary and primary organic tracer data, J. Geophys. Res.-Atmos., 115, D16204, https://doi.org/10.1029/2009JD012498, 2010.

Hu, D. and Yu, J. Z.: Secondary organic aerosol tracers and malic acid in Hong Kong: Seasonal trends and origins, Environ. Chem., 10, 381–394, https://doi.org/10.1071/EN13104, 2013.

Huang, R. J., Zhang, Y., Bozzetti, C., Ho, K. F., Cao, J. J., Han, Y., Daellenbach, K. R., Slowik, J. G., Platt, S. M., and Canonaco, F.: High secondary aerosol contribution to particulate pollution during haze events in China, Nature, 514, 218−222, https://doi.org/10.1038/nature13774, 2014.

Huang, X., Ding, A., Wang, Z., Ding, K., Gao, J., Chai, F., and Fu, C.: Amplified transboundary transport of haze by aerosol–boundary layer interaction in China, Nat. Geosci., 13, 428–434, https://doi.org/10.1038/s41561-020-0583-4, 2020.

Huang, X. H. H., Bian, Q., Ng, W. M., Louie, P. K. K., and Yu, J. Z.: Characterization of $PM_{2.5}$ major components and source investigation in suburban Hong Kong: a one year monitoring study, Aerosol Air Qual. Res., 14, 237–250, https://doi.org/10.4209/aaqr.2013.01.0020, 2014.

https://doi.org/10.5194/egusphere-2023-1835
Preprint. Discussion started: 22 September 2023

Huang, X. H. H., Bian, Q. J., Louie, P. K. K., and Yu, J. Z.: Contributions of vehicular carbonaceous aerosols to $PM_{2.5}$ in a roadside environment in Hong Kong, Atmos. Chem. Phys., 14, 9279–9293, https://doi.org/10.5194/acp-14-9279-2014, 2014.

Huo, Y. X., Guo, H., Lyu, X. P., and Yao, D. W.: Emission characteristics, sources, and airborne fate of speciated organics in particulate matters in a Hong Kong residence. Indoor Air, 32, 13017, https://doi.org/10.1111/ina.13017, 2022.

Huo, Y. X., Lyu, X. P., Yao, D. W., Zhou, B. N., Yuan, Q., Lee, S. C., and Guo, H.: Exploring the chemistry behind high levels of hydroxyl dicarboxylic acids at a coastal site in Hong Kong. NPJ Clim. Atmos. Sci., under review, 2023.

Jang, M. and McDow, S. R.: Products of benz[a]anthracene photodegradation in the presence of known organic constituents of atmospheric aerosols, Environ. Sci. Technol., 31, 1046–1053, https://doi.org/10.1021/es960559s, 1997.

Jimenez, J. L., Canagaratna, M. R., Donahue, N. M., Prevot, A. S., Zhang, Q., Kroll, J. H., DeCarlo, P. F., Allan, J. D., Coe, H., and Ng, N. L.: Evolution of organic aerosols in the atmosphere, Science, 326, 1525−1529, https://doi.org/10.1126/science.1180353, 2009.

Kanakidou, M., Seinfeld, J. H., Pandis, S. N., Barnes, I., Dentener, F. J., Facchini, M. C., Van Dingenen, R., Ervens, B., Nenes, A., Nielsen, C. J., Swietlicki, E., Putaud, J. P., Balkanski, Y., Fuzzi, S., Horth, J., Moortgat, G. K., Winterhalter, R., Myhre, C. E. L., Tsigaridis, K., Vignati, E., Stephanou, E. G., and Wilson, J.: Organic aerosol and global climate modelling: a review, Atmos. Chem. Phys., 5, 1053–1123, https://doi.org/10.5194/acp-5-1053-2005, 2005.

Kang, M. J., Fu, P. Q., Aggarwal, S. G., Kumar, S., Zhao, Y., Sun, Y. L., and Wang, Z. F.: Size distributions of n-alkanes, fatty acids and fatty alcohols in springtime aerosols from New Delhi, India, Environ. Pollut., 219, 957–966, https://doi.org/10.1016/j.envpol.2016.09.077, 2016a.

Kawamura, K., Ishimura, Y., and Yamazaki, K.: Four years' observations of terrestrial lipid class compounds in marine aerosols from the western North Pacific, Global Biogeochem. Cy., 17, 1–19, https://doi.org/10.1029/2001GB001810, 2003.

Kleindienst, T. E., Conver, T. S., McIver, C. D., and Edney, E. O.: Determination of secondary organic aerosol products from the photooxidation of toluene and their implications in ambient $PM_{2.5}$, J. Atmos. Chem., 47, 79–100, https://doi.org/10.1023/B:JOCH.0000012305.94498.28, 2004.

Lee, B. P., Li, Y. J., Yu, J. Z., Louie, P. K., and Chan, C. K.: Characteristics of submicron particulate matter at the urban roadside in downtown Hong Kong – Overview of 4 months of continuous high-resolution aerosol mass spectrometer measurements, J. Geophys. Res. Atmos., 120, 7040−7058, https://doi.org/10.1002/2015JD023311, 2015.

Lee, S. C., Cheng, Y., Ho, K. F., Cao, J. J., Louie, P. K. K., Chow, J. C., and Watson, J. G.: $PM_{1.0}$ and $PM_{2.5}$ characteristics in the roadside environment of Hong Kong, Aerosol Sci. Technol., 40, 157–165, https://doi.org/10.1080/02786820500494544, 2006.

Lelieveld, J., Barlas, C., Giannadaki, D., and Pozzer, A.: Model calculated global, regional and megacity premature mortality due to air pollution, Atmos. Chem. Phys., 13, 7023–7037, https://doi.org/10.5194/acp-13-7023-2013, 2013.

Li, R., Wang, Q., He, X., Zhu, S., Zhang, K., Duan, Y., Fu, Q., Qiao, L., Wang, Y., Huang, L., Li, L., and Yu, J. Z.: Source apportionment of $PM_{2.5}$ in Shanghai based on hourly organic molecular markers and other source tracers, Atmos. Chem. Phys., 20, 12047–12061, https://doi.org/10.5194/acp-20-12047-2020, 2020.

https://doi.org/10.5194/egusphere-2023-1835
Preprint. Discussion started: 22 September 2023

Li, Y. J., Lee, B. Y. L., Yu, J. Z., Ng, N. L., and Chan, C. K.: Evaluating the degree of oxygenation of organic aerosol during foggy and hazy days in Hong Kong using high-resolution time-of-flight aerosol mass spectrometry (HR-ToF-AMS), Atmos. Chem. Phys., 13, 8739–8753, https://doi.org/10.5194/acp-13-8739-2013, 2013.

Liao, K. Z. and Yu, J. Z.: Abundance and sources of benzo[a]pyrene and other PAHs in ambient air in Hong Kong: A review of 20-year measurements (1997-2016), Chemosphere, 259, 127518. https://doi.org/10.1016/j.chemosphere.2020.127518, 2020.

Liu, T., Li, Z., Chan, M., and Chan, C. K.: Formation of secondary organic aerosols from gas-phase emissions of heated cooking oils, Atmos. Chem. Phys., 17, 7333–7344, https://doi.org/10.5194/acp-17-7333-2017, 2017a.

Lyu, X. P., Guo, H., Cheng, H. R., Wang, X. M., Ding, X., Lu, H. X., Yao, D. W., and Xu, C.: Observation of SOA tracers at a mountainous site in Hong Kong: Chemical characteristics, origins and implication on particle growth, Sci. Total Environ., 605, 180-189, http://doi.org/10.1016/j.scitotenv.2017.06.161, 2017.

Lyu, X. P., Guo, H., Yao, D. W., Lu, H. X., Huo, Y. X., Xu, W., Kreisberg, N., Goldstein, A. H., Jayne, J., Worsnop, D., Tan, Y., Lee, S. C., and Wang, T.: In situ measurements of molecular markers facilitate understanding of dynamic sources of atmospheric organic aerosols, Environ. Sci. Technol., 54, 11058-11069, https://doi.org/10.1021/acs.est.0c02277, 2020.

Lyu, X. P., Huo, Y. X., Yang, J., Yao, D. W., Li, K. M., Lu, H. X., Zeren, Y., and Guo, H.: Real-time molecular characterization of air pollutants in a Hong Kong residence: Implication of indoor source emissions and heterogeneous chemistry, Indoor Air, 31, 1340-1352, https://doi.org/10.1111/ina.12826, 2021.

Nozière, B., González, N. J. D., Borg-Karlson, A.-K., Pei, Y., Redeby, J. P., Krejci, R., Dommen, J., Prevot, A. S. H., and Anthonsen, T.: Atmospheric chemistry in stereo: A new look at secondary organic aerosols from isoprene, Geophys. Res. Lett., 38, L11807, https://doi.org/10.1029/2011GL047323, 2011.

Pöschl, U.: Atmospheric aerosols: composition, transformation, climate and health effects, Angew. Chem. Int. Ed., 44, 7520–7540, https://doi.org/10.1002/anie.200501122, 2005.

Ramanathan, V., Crutzen, P. J., Kiehl, J. T., and Rosenfeld, D.: Aerosols, climate, and the hydrological cycle, Science, 294, 2119–2124, https://doi.org/10.1126/science.1064034, 2001.

Ren, H. X., Xue, M., An, Z. J., and Jiang, J. K.: Improving thermal desorption aerosol gas chromatography using a dual-trap design, J. Chromatogr. A, 1599, 247-252, https://doi.org/10.1016/j.chroma.2019.04.045, 2019.

Sang, X. F., Chan, C. Y., Engling, G., Chan, L. Y., Wang, X. M., Zhang, Y. N., Shi, S., Zhang, Z. S., Zhang, T., and Hu, M.: Levoglucosan enhancement in ambient aerosol during springtime transport events of biomass burning smoke to Southeast China, Tellus B, 63, 129–139, https://doi.org/10.1111/j.1600-0889.2010.00515.x, 2011.

Shen, R.-Q., Ding, X., He, Q.-F., Cong, Z.-Y., Yu, Q.-Q., and Wang, X.-M.: Seasonal variation of secondary organic aerosol tracers in Central Tibetan Plateau, Atmos. Chem. Phys., 15, 8781–8793, https://doi.org/10.5194/acp-15-8781-2015, 2015.

Simoneit, B. R. T., Kobayashi, M., Mochida, M., Kawamura, K., and Huebert, B. J.: Aerosol particles collected on aircraft flights over the northwestern Pacific region during the ACE-Asia campaign: composition and major sources of the organic compounds, J. Geophys. Res., 109, D19S09, https://doi.org/10.1029/2004JD004565, 2004.

https://doi.org/10.5194/egusphere-2023-1835
Preprint. Discussion started: 22 September 2023

Sun, C., Lee, B. P., Huang, D., Jie Li, Y., Schurman, M. I., Louie, P. K. K., Luk, C., and Chan, C. K.: Continuous measurements at the urban roadside in an Asian megacity by Aerosol Chemical Speciation Monitor (ACSM): particulate matter characteristics during fall and winter seasons in Hong Kong, Atmos. Chem. Phys., 16, 1713–1728, https://doi.org/10.5194/acp-16-1713-2016, 2016.

Sun, Y., Xu, W., Zhang, Q., Jiang, Q., Canonaco, F., Prévôt, A. S. H., Fu, P., Li, J., Jayne, J., Worsnop, D. R., and Wang, Z.: Source apportionment of organic aerosol from 2-year highly time-resolved measurements by an aerosol chemical speciation monitor in Beijing, China, Atmos. Chem. Phys., 18, 8469–8489, https://doi.org/10.5194/acp-18-8469-2018, 2018.

Sun, Y.-L., Zhang, Q., Schwab, J. J., Demerjian, K. L., Chen, W.-N., Bae, M.-S., Hung, H.-M., Hogrefe, O., Frank, B., Rattigan, O. V., and Lin, Y.-C.: Characterization of the sources and processes of organic and inorganic aerosols in New York city with a high-resolution time-of-flight aerosol mass apectrometer, Atmos. Chem. Phys., 11, 1581–1602, https://doi.org/10.5194/acp-11-1581-2011, 2011.

Surratt, J. D., Chan, A. W. H., Eddingsaas, N. C., Chan, M. N., Loza, C. L., Kwan, A. J., Hersey, S. P., Flagan, R. C., Wennberg, P. O. and Seinfeld, J. H.: Reactive intermediates revealed in secondary organic aerosol formation from isoprene, Proc. Natl. Acad. Sci. U. S. A., 107, 6640–6645, https://doi.org/10.1073/pnas.0911114107, 2010.

To, W. M., Yeung, L. L., and Chao, C. Y. H.: Characterisation of gas phase organic emissions from hot cooking oil in commercial kitchens, Indoor Built Environ., 9, 228–232, https://doi.org/10.1159/000057511, 2000.

Vaezzadeh, V., Zakaria, M. P., and Bong, C. W.: Aliphatic hydrocarbons and triterpane biomarkers in mangrove oyster (Crassostrea belcheri) from the west coast of Peninsular Malaysia, Mar. Pollut. Bull., 124, 33-42, https://doi.org/10.1016/j.marpolbul.2017.07.008, 2017.

Williams, B. J., Goldstein, A. H., Kreisberg, N. M., and Hering, S. V.: An in-situ instrument for speciated organic composition of atmospheric aerosols: Thermal desorption aerosol GC/MS-FID (TAG). Aerosol Sci. Tech., 40, 627-638, doi:10.1080/02786820600754631, 2006.

Williams, B. J., Goldstein, A. H., Kreisberg, N. M., and Hering, S. V.: In situ measurements of gas/particle-phase transitions for atmospheric semivolatile organic compounds. Proc. Natl. Acad. Sci. U.S.A., 107, 6676-6681, doi:10.1073/pnas.0911858107, 2010.

Wang, Q. Q., Qiao, L. P., Zhou, M., Zhu, S. H., Griffith, S., Li, L., and Yu, J. Z.: Source apportionment of $PM_{2.5}$ using hourly measurements of elemental tracers and major constituents in an urban environment: investigation of time-resolution influence, J. Geophys. Res.-Atmos., 123, 5284–5300, https://doi.org/10.1029/2017JD027877, 2018.

Wang, Q. Q., He, X., Zhou, M., Huang, D. D., Qiao, L. P., Zhu, S. H., Ma, Y. G., Wang, H. L., Li, L., Huang, C., Huang, X. H. H., Xu, W., Worsnop, D., Goldstein, A. H., Guo, H., and Yu, J. Z.: Hourly measurements of organic molecular markers in urban shanghai, china: primary organic aerosol source identification and observation of cooking aerosol aging, Acs Earth Space Chem., 4, 1670–1685, https://doi.org/10.1021/acsearthspacechem.0c00205, 2020.

https://doi.org/10.5194/egusphere-2023-1835
Preprint. Discussion started: 22 September 2023

Wang, Q. Q., and Yu, J. Z.: Ambient measurements of heterogeneous ozone oxidation rates of oleic, elaidic, and linoleic acid using a relative rate constant approach in an urban environment, Geophys. Res. Lett., 48, 095130, https://doi.org/10.1029/2021GL095130, 2021.

Wang, Q., Wang, S., Cheng, Y. Y., Chen, H., Zhang, Z., Li, J., Gu, D., Wang, Z., and Yu, J. Z.: Chemical evolution of secondary organic aerosol tracers during high-$PM_{2.5}$ episodes at a suburban site in Hong Kong over 4 months of continuous measurement, Atmos. Chem. Phys., 22, 11239–11253, https://doi.org/10.5194/acp-22-11239-2022, 2022.

Wang, Y., Wang, H., Guo, H., Lyu, X., Cheng, H., Ling, Z., Louie, P. K. K., Simpson, I. J., Meinardi, S., and Blake, D. R.: Long-term O3–precursor relationships in Hong Kong: field observation and model simulation, Atmos. Chem. Phys., 17, 10919–10935, https://doi.org/10.5194/acp-17-10919-2017, 2017.

Wong, Y.K., Huang, X.H.H., Cheng, Y.Y., Louie, P.K.K., Yu, A.L.C., Tang, A.W.Y., Chan, D.H.L., and Yu, J.Z.: Estimating contributions of vehicular emissions to $PM_{2.5}$ in a roadside environment: a multiple approach study, Sci. Total Environ., 672, 776–788, https://doi.org/10.1016/j.scitotenv.2019.03.463, 2019.

Xing, L., Fu, T. M., Liu, T. Y., Qin, Y. M., Zhou, L. Y., Chan, C. K., Guo, H., Yao, D. W., and Duan, K. Q.: Estimating organic aerosol emissions from cooking in winter over the Pearl River Delta region, China, Environ. Pollut., 292, 118266, https://doi.org/10.1016/j.envpol.2021.118266, 2022.

Yang, Y., Tang, R., Qiu, H., Lai, P. C., Wong, P., Thach, T. Q., Allen, R., Brauer, M., Tian, L. W., and Barratt, B.: Long term exposure to air pollution and mortality in an elderly cohort in Hong Kong, Environ. Int., 117, 99–106, https://doi.org/10.1016/j.envint.2018.04.034, 2018.

Yao, D. W., Lyu, X. P., Lu, H. X., Zeng, L. W., Liu, T. Y., Chan, C. K., and Guo H.: Characteristics, sources and evolution processes of atmospheric organic aerosols at a roadside site in Hong Kong, Atmos. Environ., 118298, https://doi.org/10.1016/j.atmosenv.2021.118298, 2021.

Yao, D. W., Guo, H., Lyu, X. P., Lu, H. X., and Huo, Y. X.: Secondary organic aerosol formation at an urban background site on the coastline of South China: Precursors and aging processes, Environ. Pollut., 309, 119778, https://doi.org/10.1016/j.envpol.2022.119778, 2022.

Yao, X. H., Fang, M., Chan, C. K., Ho, K. F., and Lee, S. C.: Characterization of dicarboxylic acids in $PM_{2.5}$ in Hong Kong, Atmos. Environ., 38, 963-970, https://doi.org/10.1016/j.atmosenv.2003.10.048, 2004.

Yu, J. Z., Huang, X. H., Ho, S. S., and Bian, Q.: Nonpolar organic compounds in fine particles: quantification by thermal desorption-GC/MS and evidence for their significant oxidation in ambient aerosols in Hong Kong, Anal. Bioanal. Chem., 401, 3125–3139, https://doi.org/10.1007/s00216-011-5458-5, 2011.

Zeng, J., Yu, Z., Mekic, M., Liu, J., Li, S., Loisel, G., Gao, W., Gandolfo, A., Zhou, Z., Wang, X., Herrmann, H., Gligorovski, S., and Li, X.: Evolution of indoor cooking emissions captured by using secondary electrospray ionization high-resolution mass spectrometry, Environ. Sci. Techn. Let., 7, 76–81, https://doi.org/10.1021/acs.estlett.0c00044, 2020.

https://doi.org/10.5194/egusphere-2023-1835
Preprint. Discussion started: 22 September 2023

Zhang, Q., Zheng, Y., Tong, D., Shao, M., Wang, S., Zhang, Y., Xu, X., Wang, J., He, H., and Liu, W.: Drivers of improved $PM_{2.5}$ air quality in China from 2013 to 2017, Proc. Natl. Acad. Sci. U. S. A., 116, 24463−24469, https://doi.org/10.1073/pnas.1907956116, 2019.

Zhang, Y. N., Zhang, Z. S., Chan, C. Y., Engling, G., Sang, X. F., Shi, S., and Wang, X. M.: Levoglucosan and carbonaceous species in the background aerosol of coastal southeast China: case study on transport of biomass burning smoke from the Philippines, Environ. Sci. Pollut. Res., 19, 244–255, https://doi.org/10.1007/s11356-011-0548-7, 2012.

Zielinska, B., Sagebiel, J., McDonald, J. D., Whitney, K., and Lawson, D. R.: Emission rates and comparative chemical composition from selected in-use diesel and gasoline-fueled vehicles, J. Air Waste Manage. Assoc., 54, 1138−1150, https://doi.org/10.1080/10473289.2004.10470973, 2004.

https://doi.org/10.5194/egusphere-2023-1835
Preprint. Discussion started: 22 September 2023

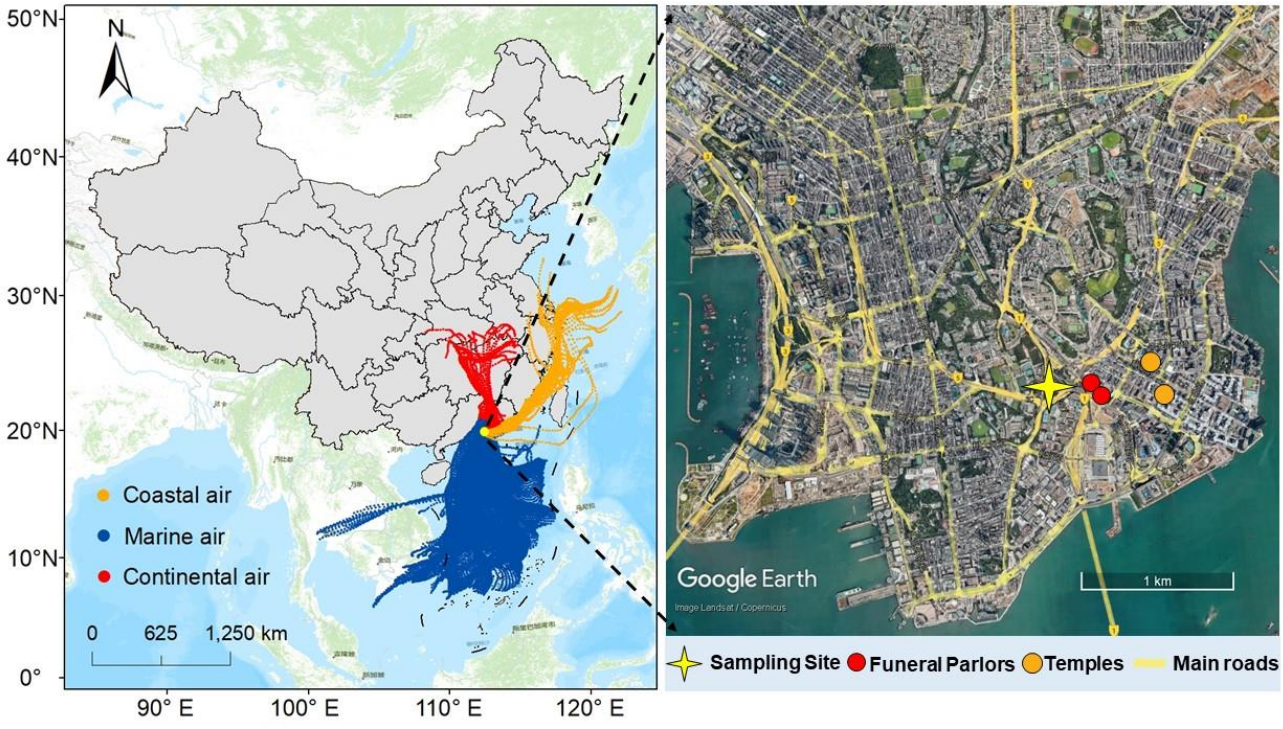

Figure 1: Location of the sampling site and the surrounding environment. Background maps are adapted from ArcGIS and © Google Earth.

https://doi.org/10.5194/egusphere-2023-1835
Preprint. Discussion started: 22 September 2023

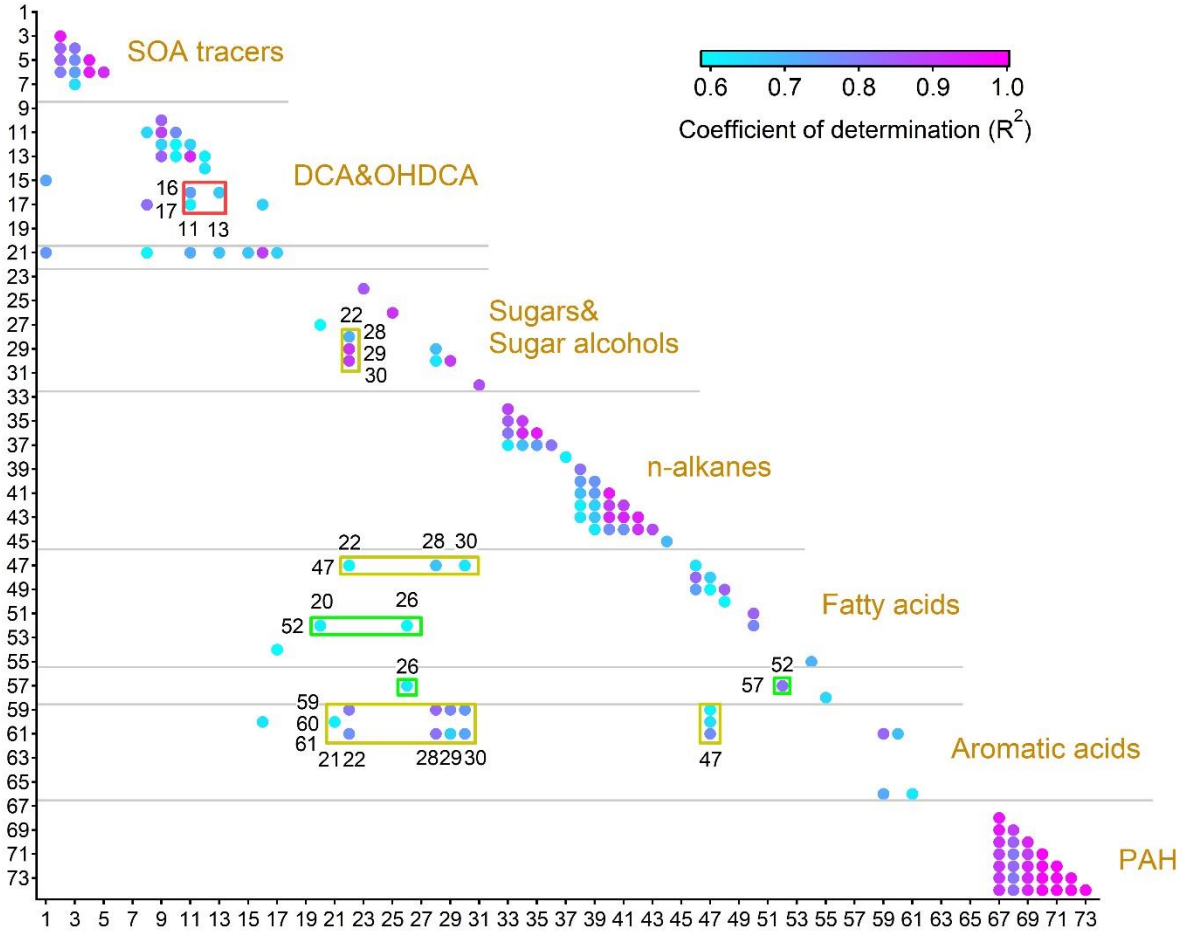

1 2-MGA
2 2-MT1
3 2-MT2
4 cis-2-MBT
5 3-MBT
6 *trans*-2-MBT
7 HDMGA
8 DHOPA
9 TA1
10 TA2
11 MA
12 CMA
13 2-HGA
14 2-hydroxydicarboxylic acid
15 Succinic acid
16 Fumaric acid
17 Glutaric acid
18 Pimelic acid
19 Adipic acid
20 Azelaic acid
21 Glyceric acid
22 Hydroxybutyric acid
23 Mannose
24 Glucose
25 Fructose-1
26 Fructose-2
27 Xylose
28 Levoglucosan
29 Mannosan
30 Erythritol
31 Arabinitol
32 Mannitol
33 *n*-C_{20}
34 *n*-C_{21}
35 *n*-C_{22}
36 n-C_{23}
37 *n*-C_{24}
38 *n*-C_{25}
39 *n*-C_{26}
40 n-C_{27}
41 *n*-C_{28}
42 *n*-C_{29}
43 *n*-C_{30}
44 n-C_{31}
45 *n*-C_{32}
46 Capric acid
47 Undecylic acid
48 Lauric acid
49 Tridecylic acid
50 Myristic acid
51 Pentadecylic acid
52 Palmitic acid
53 Stearic acid
54 Underivatized palmitic acid
55 Underivatized stearic acid
56 Norhopane
57 Oleic acid
58 Underivatized oleic acid
59 VA
60 3-OHBA
61 4-OHBA
62 Phthalic acid
63 Isophthalic acid
64 Terephthalic acid
65 2,4-dyhydroxybenzoic acid
66 Protocatechuic acid
67 Fluoranthene
68 Pyrene
69 Benzo [*a*] anthracene
70 Chrysene triphenylene
71 Benzo [*e*] pyrene
72 Benzo [*a*] pyrene
73 Benzo [*b*] fluoranthene
74 Benzo [*k*] fluoranthene

Figure 2: Correlations between OA molecular markers with R^2 not lower than 0.6. Bold are the representative species that we focus on in this study. Full names of the abbreviations are given in Table S2.

https://doi.org/10.5194/egusphere-2023-1835
Preprint. Discussion started: 22 September 2023

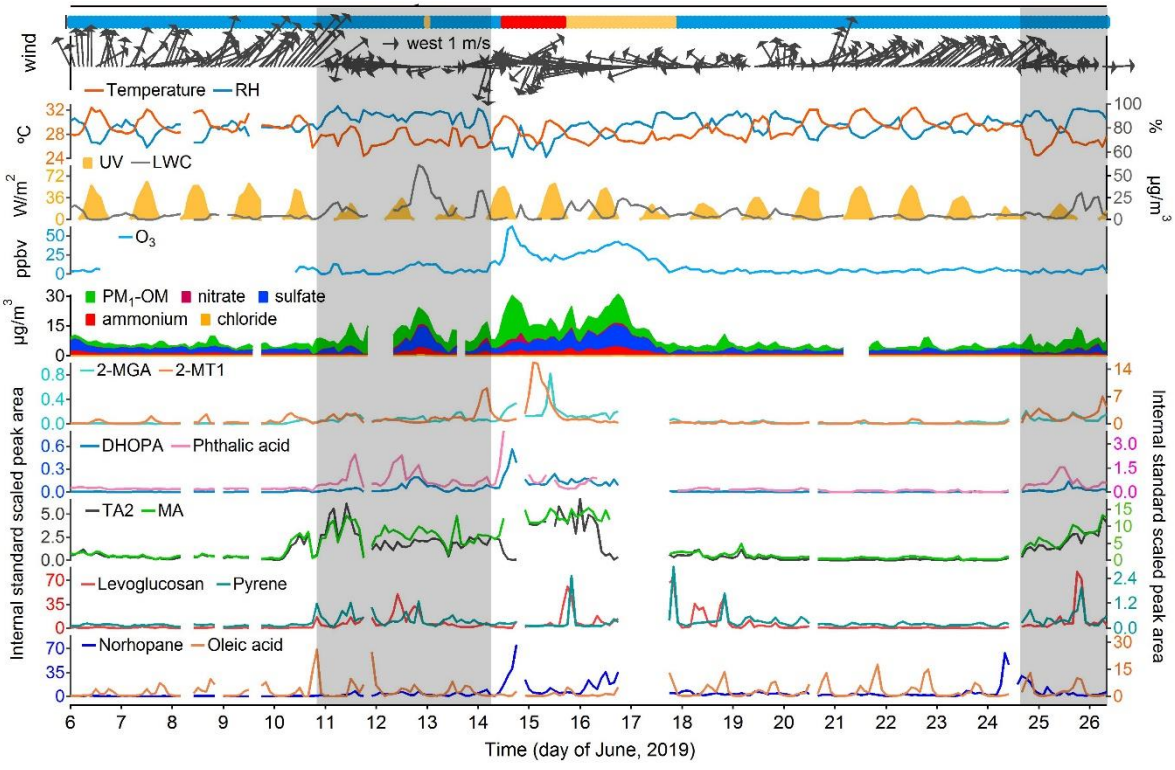

Figure 3: Time series of representative OA markers, PM_1 compositions, trace gases, and meteorological conditions. Blue, orange, and red bars at the top represent marine, coastal, and continental air, respectively. Shaded areas represent the periods with troughs. Missing data are due to instrument maintenance.

https://doi.org/10.5194/egusphere-2023-1835
Preprint. Discussion started: 22 September 2023

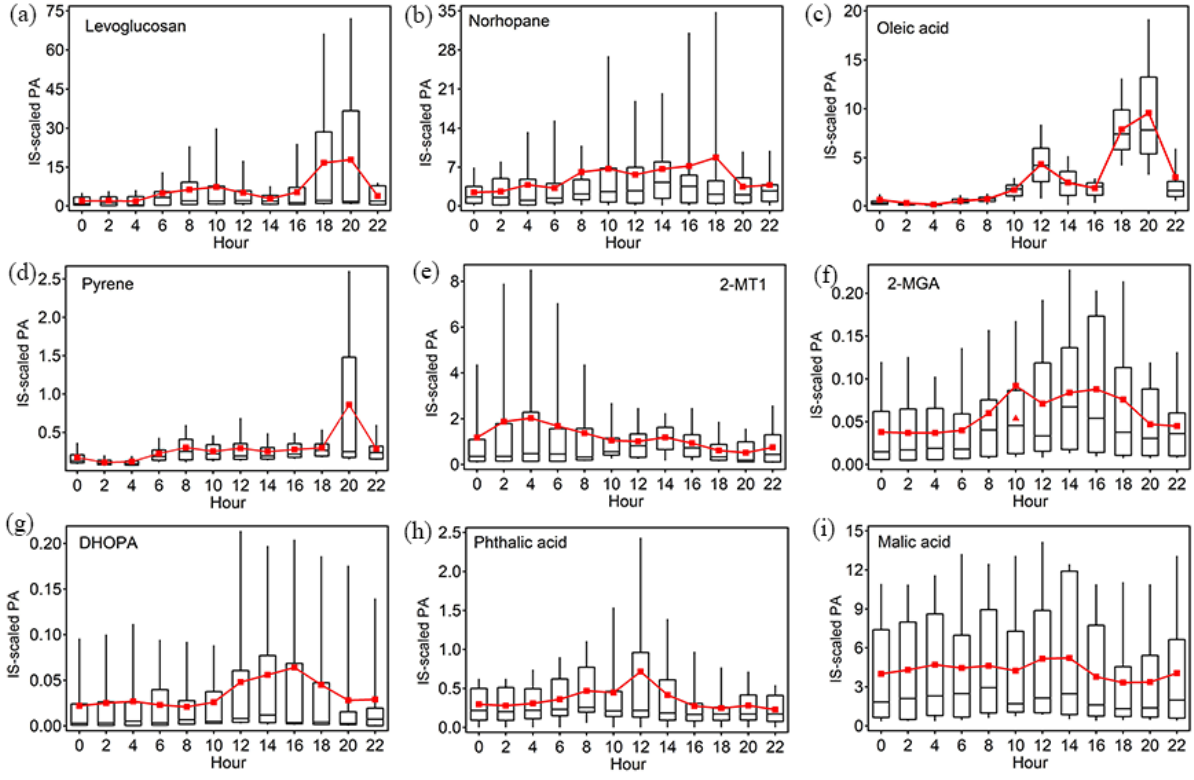

Figure 4: Average diurnal patterns of nine representative OA markers. Tip of the top (bottom) whisker is the 95th (5th) percentile. Top and bottom of the box denote the 75th and 25th percentiles, respectively. Line inside the box represents the median value, and the mean value is indicated by red square and triangle (excluding data on June 14th – 15th for 2-MGA only).

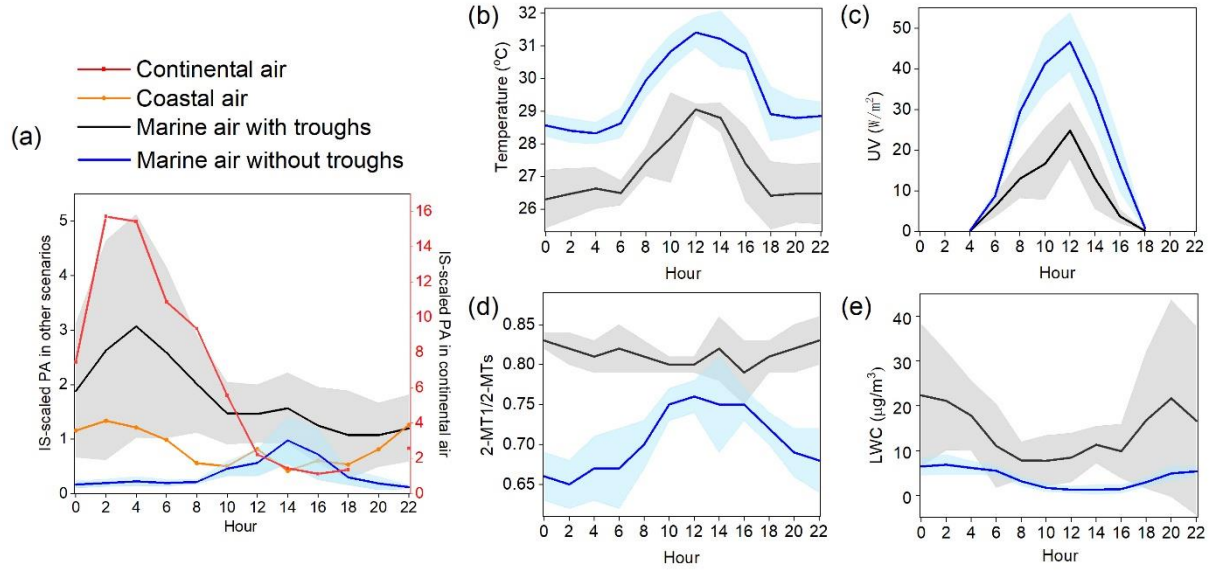

https://doi.org/10.5194/egusphere-2023-1835
Preprint. Discussion started: 22 September 2023

Figure 5: Diurnal patterns of 2-MT1 in different scenarios (a) and the comparisons of temperature (b), UV (c), 2-MT1/2-MTs ratio (d), and LWC (e) between the marine air with and without troughs. Shaded areas represent 95% confidence intervals.

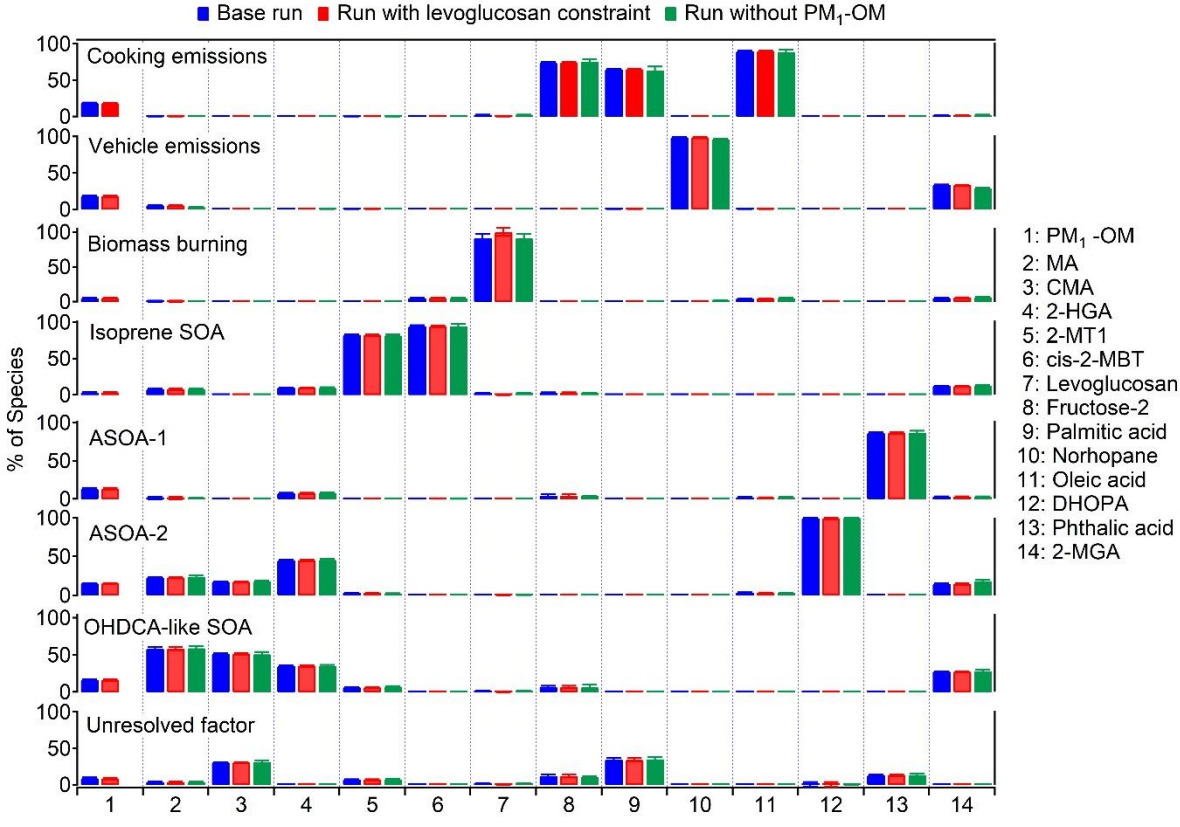

Figure 6: Average profiles of the eight factors resolved by PMF. The error bars represent 95% confidence intervals estimated by the BS method.

https://doi.org/10.5194/egusphere-2023-1835
Preprint. Discussion started: 22 September 2023

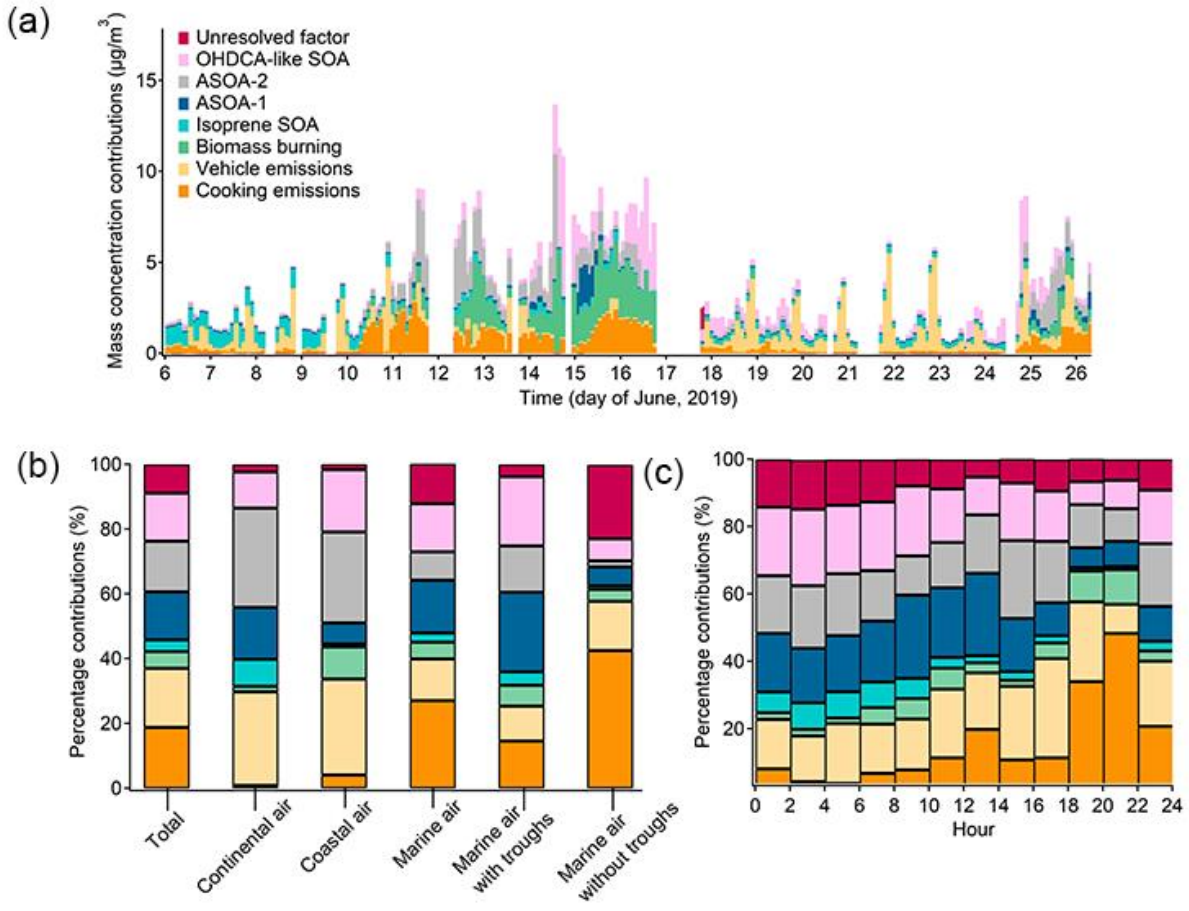

Figure 7: Contributions of individual OA sources to PM_1-OM: time series of bihourly data (a); averages for the scenarios of different air masses (b); and diurnal variations (c).